

AIRBORNE DOPPLER OBSERVATIONS OF A CONVECTIVE SYSTEM OVER THE EASTERN ALPS DURING MAP IOP5

Cheng-Ku Yu¹, Frank Roux², and David P. Jorgensen³

¹Department of Atmospheric Sciences, National Taiwan University, Taipei, Taiwan

²Laboratoire d'Aérodologie (CNRS-UPS), Toulouse, France

³NOAA/National Severe Storms Laboratory, Boulder, Colorado, USA

1. INTRODUCTION

Relevant dynamics of terrain influence in the presence of steady, horizontally uniform onshore flow have been explored to some degree by previous studies. However, interactions of unsteady, diabatic flow with topography remain largely unexplored. Under suitable environmental conditions such interaction can result in the development of locally intense rainfall and high surface winds in the vicinity of the mountains. Unfortunately, the lack of detailed observations nearby topography has largely limited our knowledge of the severe weather conditions and underlying dynamical processes accompanying the orographic modification of these events. Special measurements, including in-situ and Doppler radar data, collected from instrumented aircraft during the MAP (Mesoscale Alpine Program) special observing period (Bougeault et al. 2001) provide highly detailed views of airflow and precipitation not only farther upstream but also directly over the inland sloped terrain. This allows us to explore our knowledge of processes associated with orographically influenced precipitation.

During MAP IOP5, a convective system was initiated at ~0500 UTC 4 October 1999 over the mountainous regions near the border of northern Italy and western Slovenia while a synoptic cold front (upper-level trough) approached the eastern edge (middle part) of the Alps. As revealed by a sequence of ground-based radar observations at Fossalon (location refers to Fig. 1), the precipitation within the system developed into a highly organized feature within the next 3 hours, characterized by a narrow but intense band extending from the inland sloped terrain to a location well far upstream of topography over the northern Adriatic Sea. During the period, both NCAR Electra and NOAA P-3 aircraft made comprehensive Doppler observations over the northern portion of the convective system as it advanced eastward and interacted increasingly with the mountains. The main objective of this study is to use airborne Doppler radar observations to document the airflow and precipitation structure of the mountainous convective system and to investigate the possible roles of topography in influencing the development of this system.

2. AUTOMATED EDITING PROCEDURE

In contrast to the airborne Doppler measurements collected over the ocean or a relatively flat surface for ne-

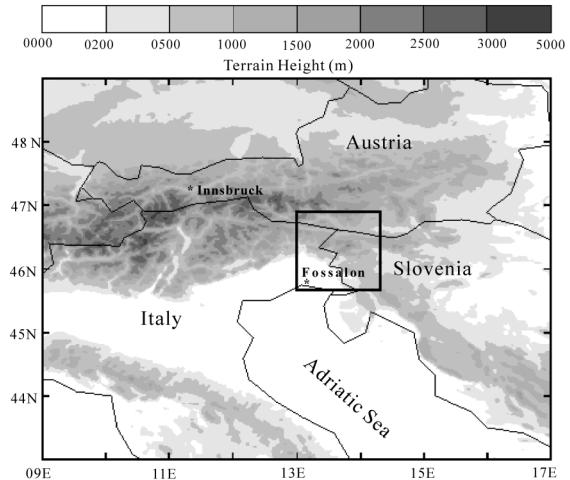


Fig. 1. Topography in the eastern portion of Alps. Terrain height (m MSL) is indicated by shading (key at top). The inset square denotes the dual-Doppler analysis domain (120X120 km²).

arly all of the previous field experiments, MAP airborne Doppler radar data, particularly for the event studied herein, was gathered primarily over the mountainous regions. Hence, the raw radar data appear to contain considerable nonmeteorological radar echoes, such as mountain clutter and second-trip echo, exclusively related to the local topographic features. In this study, an automated editing procedure was developed to remove these different types of contamination. For the ground/mountain clutter removal, the altitudes of each range gate are calculated and then compare it to a high-resolution (30 seconds) digital topographic dataset. Once a range gate along the radar bin is found to be lower than the surface elevation, remaining gates beyond it are all considered to be the mountain clutter and thus removed. In principle, such removal method would work well as long as uncertainties associated with the errors of the Inertial Navigation System (INS), such as pointing angles and aircraft position, could be well taken into account. Hence, a technique of deducing these navigation errors proposed by Georgis et al. (1999) was also applied to complement the automated procedure, which allows for a better determination of each gate locations relative to the topography. Contamination due to the second-trip echo is pretty common for MAP airborne Doppler radar data. In the automated procedure, the

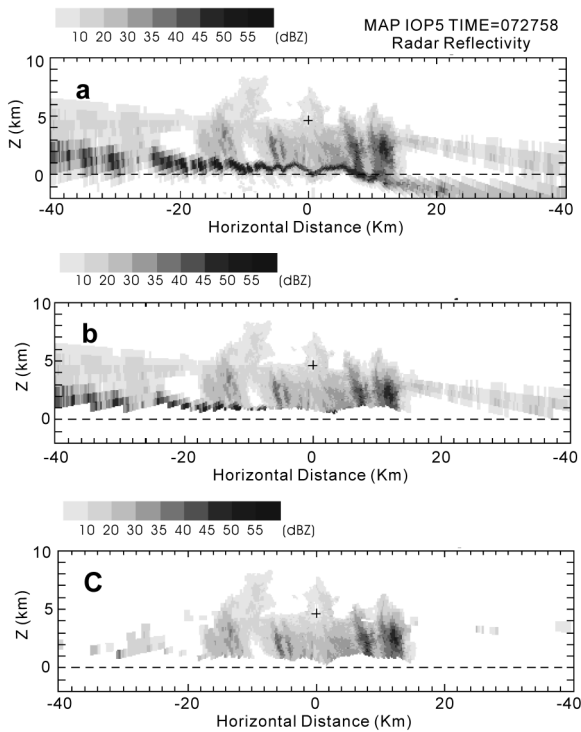


Fig. 2. Vertical cross sections of radar reflectivity (dBZ) constructed from 360 degree sweeps of the X-band Doppler radar aboard the NCAR Electra at 0727 UTC 4 October 1999 during MAP IOP5. (a) Raw data without applying any editing procedure. (b) Product after removing those gates below heights of the mountain, however without taking the INS errors into account. (c) Final product after applying the automated editing procedure developed in this study. The aircraft position is indicated by + at an altitude near 4668 m (MSL).

second-trip echo is identified based on the gradient of radial velocities in the alongbeam direction. The radar echoes are considered as second-trip echo when the calculated alongbeam gradient, in which the elevations of radar beams are within $\pm 20^\circ$ from the horizontal, exceeds an arbitrary value (0.04 s^{-1} chosen for this case) within the five consecutive gates. Additionally, gates of radial velocity having unreasonable magnitude and alongbeam discontinuity are also precluded in this automated procedure.

In order to evaluate the capability of the automated editing procedure, vertical cross sections of radar reflectivity constructed from individual 360° sweeps of the X-band Doppler radar were examined with (without) applying this procedure. An example of vertical section plots from a fore scanning of the NCAR Electra airborne Doppler radar to illustrate the results of the automated editing procedure is shown in Fig. 2. There were considerable mountain clutter near the ground surface and second-trip echoes on the both sides of aircraft as seen in the plot of raw radar sweep data (Fig. 2a). When applying the editing procedure without, however, the correction of INS errors, some mountain clutter still could be found on the left of the aircraft and below the aircraft (Fig. 2b). The INS errors retrieved from the Doppler leg 0720-0725 UTC were then taken into account to recalculate the location of each gate. For this leg, the correction values for roll, pitch, heading, range delay (aft scanning), range delay (fore scanning) and radar location (x,y,z) were equal to -1.9° , -1.2° , -0.01° , 191 m, 292 m, -1286 m, -886 m, and 5 m, respectively. When these INS corrections were incorporated into the procedure and removal scheme of second-trip echo were also applied, nearly all clutters could be successfully removed as shown in Fig. 2c.

3. DUAL-DOPPLER SYNTHESIS RESULTS

In this study, three-dimensional airflow within the convective system is obtained by use of a pseudo-dual-Doppler synthesis derived from multiple-view radial velocity data as described by Jorgensen and Smull (1993). The horizontal and vertical analysis grid spacing were set to 1.5 km and 0.25 km, respectively, over a volume encompassing $120 \times 120 \text{ km}^2$ in the horizontal and 12 km in the vertical. The location of dual-Doppler analysis domain is shown by the inset box in Fig. 1. Vertical air motions were obtained through an iterative procedure by assuming anelastic continuity through downward integration from an upper-boundary condition of zero vertical motion at echo top. In this computation, the variational adjustment scheme described by O'Brien (1970) was also applied to compensate for divergence errors that produce nonzero vertical motions at the ground.

Figure 3 shows the horizontal airflow and precipitation structure at 2.5 and 4.5 km (MSL) derived from an early Doppler leg of NCAR Electra at 0727 UTC. During this period, convection within the system was organized into a narrow zone of high radar reflectivities with a maximum greater than 45 dBZ. The narrow band was oriented approximately south-north. At low levels, the southwesterly flow prevailed along the precipitation band. A vertical cross section normal to the band (along $Y = 48 \text{ km}$) indicates a strong convective nature, with the 40 dBZ contour extending to a height of 4-5 km MSL (Fig. 4a). The regions of the convective cores were predominantly upward motions with maximum Doppler-derived updraft velocities of $4\text{-}5 \text{ ms}^{-1}$. There was an evidence of northerly flow observed near the northern end of the band (Fig. 3a) over the higher terrain. No presence of the northerly flow observed at low levels was seen at higher levels (cf. Fig. 3b). The flow was, in fact, confined to below 3 km and would be probably originated to the north of the Alps. In contrast to the vertical structure shown in Fig. 4a, the region of having northerly flow component was dominated by stratiform precipitation and was characterized by weaker downward (upward) air motions below (above) the melting level ($\sim 3 \text{ km MSL}$) (Fig. 4b). Note that at this time, considerable convection characterized by multiple centers of heavy precipitation was also evident ahead of the precipitation band (Fig. 3b). These cells existed over a relatively steep mountain slope, and in particular, aligned in the direction parallel to the low-level prevailing southwesterly flow. It is suggested that their generation would be related to the processes in association with the upslope forcing.

4. CONCLUSIONS

Airborne Doppler radar measurements were used to document the detailed structure of a convective system that developed over the mountainous regions near the border of northern Italy and western Slovenia on 4 October 1999 during MAP IOP5. Results from the initial Doppler observations revealed complicated features of precipitation within the system. Our analyses suggest that, in addition to the convective forcing associated with the synoptic cold front, moist and unstable prevailing southwesterly flow interacting with the sloped terrain would also play an important role in the generation of precipitation particularly ahead of the major precipitation band. Examination of other available airborne Doppler observations collected during the later periods by both NCAR Electra and NOAA P-3 aircraft will be required for

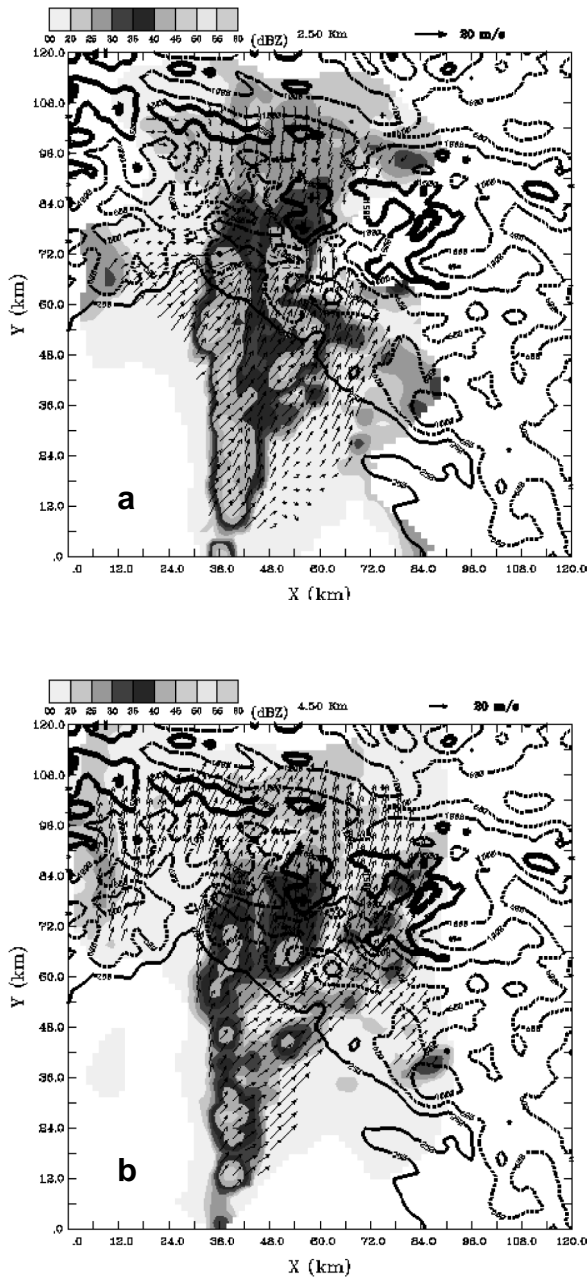


Fig. 3. Ground-relative winds (indicated by wind vectors, key at upper right) and radar reflectivity (dBZ, key to shading at upper left) at 2.5 km (a) and 4.5 km (b) derived from the airborne dual-Doppler analysis at 0727 UTC. In each panel, terrain height thresholds of 250, 600, 1000, 1500 and 2000 m MSL are indicated by solid, dashed, dashed-dotted, thick-solid and dark thick-solid contours, respectively.

better understanding of orographic impact on this convective system as it further encountered the regions of higher inland terrain.

Acknowledgments. We thank the efforts of the NCAR Electra and NOAA P-3 flight crews for their dedication and support during MAP. Financial support for the first author to participate in the MAP flight mission was provided by the National Science Council of the Republic of China. This research has been supported by the National Science Council of the Republic of China under Grant NSC90-2119-M-002-004.

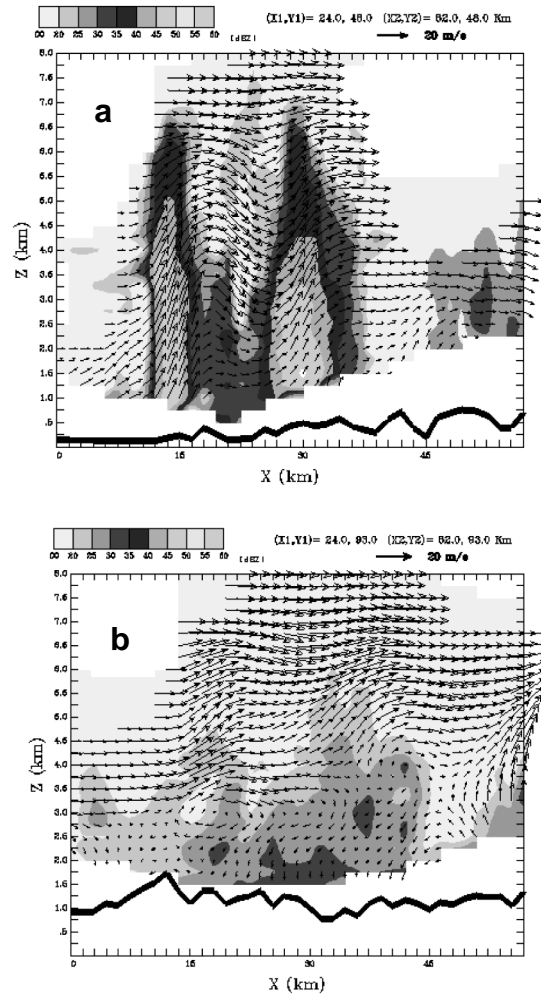


Fig. 4. East-west vertical cross section of ground-relative winds and radar reflectivity (key at upper left) approximately normal to the precipitation band at (a) $Y=48$ km and (b) $Y=93$ km in Fig. 3. Heavy solid line in lower portion of each panel indicates height of topography along the section.

REFERENCES

- Bougeault P., P. Binder, A. Buzzi, R. Dirks, R. Houze, J. Kuettner, R. B. Smith, R. Steinacker, and H. Volkert, 2001: The MAP Special Observing Period. *Bull. Amer. Meteor. Soc.*, **82**, 433-462.
- Georgis J.- F., F. Roux, and P. H. Hildebrand, 1999: Observation of precipitating systems over complex orography with meteorological Doppler radars: A feasibility study. *Meteor. Atmos. Phys.*, **72**, 185-202.
- Jorgensen, D. P., and B. F. Smull, 1993: Mesovortex circulations seen by airborne Doppler radar within a bow-echo mesoscale convective system. *Bull. Amer. Meteor. Soc.*, **74**, 2146-2157.
- O'Brien, J. J., 1970: Alternative solutions to the classical vertical velocity problem. *J. Appl. Meteor.*, **9**, 197-203.